Available online at www.sciencedirect.com
ScienceDirect
Progress in Natural Science 19 (2009) 1493–1499
Progress in Natural Science
www.elsevier.com/locate/pnsc

Sodium current of neurosecretory cells in the eyestalk from the shrimp *Penaeus japonicus*

Jinshen Liu [a], Shiying Li [b], Haihui Ye [a,*], Guizhong Wang [c]

[a] *Department of Oceanography, Xiamen University, Xiamen 361005, China*
[b] *Xiamen Institute of Medicine, Xiamen 361003, China*
[c] *State Key Laboratory of Marine Environment Science, Xiamen 361005, China*

Received 18 February 2009; received in revised form 17 March 2009; accepted 7 April 2009

Abstract

The properties of the inward current of medulla terminalis-X-organ (MTXO) cells isolated from the *Penaeus japonicus* eyestalk were studied with the whole-cell clamp technique in the presence of Ca^{2+} and K^+ channel blockers. The inward currents had a threshold at about −50 mV and peaked at −10 mV. The reversed potential (V_{rev}) was very close to V_{Na}, the theoretical Nernst equilibrium potential for Na^+. V_{rev} followed V_{Na} when the external Na^+ concentration was varied and the currents were entirely suppressed by 30 nM tetrodotoxin (TTX), indicating that it was carried by Na^+. The smooth line of concentration-dependent inhibition of sodium currents by TTX represented the best fit with the Hill equation, yielding an IC_{50} of 2.1 ± 0.1 nM. The values of the half-maximal activation voltage V_h were −20.6 ± 0.5 and −19.3 ± 0.5 mV, respectively, in the absence and presence of 2 nM TTX. TTX had no significant effect on the voltage dependence of steady-state activation and inactivation of I_{Na}. Taken together, the results suggest that the inward current recorded under our experimental conditions was carried by sodium ions flowing through fast voltage-dependent Na^+ channels.

Keywords: MTXO; Sodium current; *Penaeus japonicus*; Patch–clamp

1. Introduction

The neurosecretory system of the crustacean eyestalk, known as the X-organ-sinus gland (XOSG) system, is the major neurosecretory apparatus in crustaceans, analogous to the vertebrate hypothalamo-neurohypophyseal system [1]. A conglomerate of 150–200 neurosecretory somata located in the medulla terminalis of the eyestalk (MTXO). At least eight hormones, such as the molt-inhibiting hormone (MIH), the gonad-inhibiting hormone (GIH) and the crustacean hyperglycemic hormone (CHH), appear to be synthesized in the X-organ. The hormones are subsequently transported along axons which end as bulbous terminals in close apposition to a blood sinus, forming a neurohaemal organ, the sinus gland, near the medulla external of the eyestalk [2]. The X-organ hormones regulate a host of physiological functions such as tegumentary and retinal pigment position, gonad activity, molting, blood sugar level, locomotion and neuronal activity. They are all of a peptidic nature. Some appear to be unique to crustaceans, while others are common to various zoological groups [3–5].

Penaeus japonicus is a commercially important species in mariculture. It distributes widely throughout the Indo-West Pacific (IWP) [6]. The range covers East Asia (including the South China Sea and the Sea of Japan), Southeast Asia (including the Indonesian Archipelago), Australia (including the northern coast of Queensland and a small population near Mackay), the Red Sea and the Indian Ocean (including eastern and southern Africa) [7]. The shrimp has been farmed in Japan and China for about

* Corresponding author. Tel./fax: +86 592 2185539.
E-mail address: haihuiye@xmu.edu.cn (H. Ye).

1002-0071/$ - see front matter © 2009 National Natural Science Foundation of China and Chinese Academy of Sciences. Published by Elsevier Limited and Science in China Press. All rights reserved.
doi:10.1016/j.pnsc.2009.04.009

six decades and has been selectively bred for at least six generations. Removal of one eyestalk has been used for years to induce an accelerated ovarian maturation and spawning in *P. japonicus* [8]. In order to investigate the physiological processes involved in excitation–secretion coupling and in the regulation of neurosecretory functions, it appeared essential to determine precisely the basic ionic mechanisms involved in their cell membrane electrical activities [9].

Most of our information on the electrical properties of X-organ cells stems from studies in the four species, the lobsters (*Panulirus marginatus*), the crab (*Cardisoma carnifex*, *Eriocheir sinensis*) and the crayfish (*Procambarus clarkii*) [10–13]. Various patterns of electrical activity have been recorded from X-organ somata and neurites using the patch–clamp technique in crustaceans, such as the calcium-activated potassium current [11,12], the delayed rectifier and the transient potassium currents [13,14], the ATP-sensitive potassium current [15,16] and the GABA-gated current [17]. To our knowledge, almost nothing is known concerning the characteristics of the ionic currents and their contribution to the control of hormone secretion activities in neurosecretory cells of the shrimp, *P. japonicus*.

Voltage-gated sodium channels are plasma membrane proteins that mediate the rapid increase in Na^+ permeability during the initial phase of action potentials in nerve, neuroendocrine, skeletal muscle and heart cells [18]. The voltage-gated sodium current is the important voltage-gated ion channel to be studied, and its research has helped to understand other voltage-gated ion channels.

Therefore, it appeared necessary to characterize the kinetics of other ionic currents and, above all, those of the sodium current. In this paper, we describe the study with the patch–clamp technique of the voltage-dependent inward sodium current of the isolated X-organ neurons from *P. japonicus*.

2. Materials and methods

2.1. Cell isolation

Adult shrimp of either sex, 10–13 cm long, were obtained from local vendors in Xiamen. Eyestalks were excised and placed in a sylgard-coated Petri dish with ice-cold shrimp physiological saline solution (PSS), consisting of (in mM) NaCl 300, KCl 10, $MgCl_2$ 10, $CaCl_2$ 10, glucose 5 and Hepes 10, the pH was adjusted to 7.0 with NaOH. The formulation of PSS was modified from the report by Lang et al. [19]. The exoskeleton, muscles and connective tissue surrounding the neural structures were carefully removed under a dissecting microscope. Isolated X-organs were incubated with 1.5 mg/ml papain, 1.5 mg/ml protease I, 1.5 mg/ml dithiothreitol (DTT) and 2 mg/ml bovine serum albumin (BSA) dissolved in PSS for 15 min. The X-organs were then rinsed in enzyme-free PSS and mechanically dissociated by repetitive gentle suctions through a Pasteur pipette. The suspension was then filtered and centrifuged at 90*g* for 1 min and the pellets were resuspended in 1 ml PSS. Aliquots of this solution were added to glass cover slips previously coated with poly-D-lysine. Cells were stored at 28 °C and used within 6 h.

2.2. Electrophysiology

Patch–clamp recordings were performed using standard whole-cell voltage–clamp techniques. A piece of coverslip with neurosecretory cells was placed into a self-made recording chamber that was mounted on the stage of an inverted microscope. Most of the cells were ovoid-shaped, with diameters between 20 and 40 μm, average capacitance 27.5 PF. Only the somata of the X-organ cell without WSSV (white spot syndrome virus) were used in the experiment. Cells were superfused with a bath solution which contained (in mM) NaCl 300, TEA-Cl 10, $MgCl_2$ 10, $CaCl_2$ 10, glucose 5, $CdCl_2$ 0.2 and Hepes 10, the pH was adjusted to 7.0 with NaOH. The inclusion of TEA and Cd^{2+} in the bath solution was to minimize the contamination of potassium and calcium currents. The patch pipettes (borosilicate glass, WPI) were pulled with a Flaming Brown P-97 micropipette puller (Sutter Instruments, USA). The resistances of the pipettes ranged from 1 to 2 MΩ when filled with an internal solution containing (in mM) Hepes 10, CsCl 100, CsF 200, NaCl 15, EGTA 10, TEA-Cl 10, MgATP 1, $MgCl_2$ 2, the pH was adjusted with CsOH to 6.8. Membrane currents were recorded using the Axopatch amplifier (Axopatch 200B, Axon Instruments, Inc.). Series resistances were always compensated by 70% with the amplifier's built-in circuitry. Current signals were low pass filtered at 2 kHz, digitized at 10 kHz and the on-line leak subtracted via a P/4 protocol. Data acquisition and analysis were performed with pClamp software (version 8.24, Axon Instruments, Inc.). The amplitudes of the currents were measured from the baseline to the peak value and were normalized for cell capacitance as whole-cell current densities (pA/pF). All experiments were performed at room temperatures (22–24 °C).

2.3. Drugs and chemicals

Papain, TEA, EGTA, protease, CsCl, CsF, MgATP, DTT and Hepes were purchased from Sigma. TTX, obtained from the Hebei Institute of Aquaculture (China), was prepared as 1 mM stock solution in water and stored at −20 °C. DMSO was obtained from the Shanghai Sangon Biological Engineering Technology and Services Company. Bovine serum albumin was obtained from Bio Basic, Inc.

2.4. Statistical analysis

Data were expressed as mean ± SE. Differences in the data were evaluated by the paired *t*-test. *P* values less than 0.05 were taken as a statistically significant difference. Software Microcal Origin 7.0 was used for statistical analysis and graph plotting.

3. Results

3.1. Currents of neurosecretory cells in XOSG from eyestalks

Voltage-dependent currents were recorded in ovoid-shaped neurons dissociated from the MTXO of the eyestalk. It had two kinds of inward current and one kind of outward current.

We tried to isolate I_{Na} from the other kinds of voltage-dependent ionic currents in whole-cell patch–clamp recordings by (1) TEA were added to both the bath and pipette solution and potassium was substituted by equimolar cesium in the pipette solution to block potassium currents; (2) Cd^{2+} in the bath solution was used to minimize the contamination of calcium currents. Inward currents were evoked using the standard stimulus protocol to record the current–voltage relationship (I–V curve) of the voltage-gated ion channel. i.e. the membrane potentials were stepped to test potentials between −80 and +60 mV for 150 ms from a holding potential of −70 mV in a 10 mV increment with an interval of 10 s.

Under these conditions, depolarizing pulses activated inward currents. The amplitudes of these currents displayed a U-shaped dependence on membrane potentials between −80 and +60 mV (Fig. 1). The inward currents had a threshold at about −50 mV and peaked at −10 mV. The currents which persisted in PSS with Cd^{2+} were insensitive to 10 μM nifidipine (data not shown), indicating that L-type calcium currents are not responsible for these fast activating and fast inactivating currents. To further identify the nifidipine-insensitive currents, we studied its dependence on external Na^+ and its sensitivity to TTX.

3.2. Sodium dependence of the inward current

If the inward current is carried by Na^+, its reversal potential should change with the sodium equilibrium potential (E_{Na}). To change E_{Na}, the external sodium concentration ($[Na^+]_o$) was decreased using equimolar substitution with choline which is impermeable to sodium channels. Lowering external $[Na^+]_o$ with equimolar choline always resulted in the following effects: (1) the magnitude of the inward current was decreased, suggesting that Na^+ is the charge carrier; (2) the reversal potentials of the inward current were shifted in the negative direction as $[Na^+]_o$ was lowered, and the magnitude of the shift was consistent with the change in E_{Na}. The I_{Na} reversal potential in cells superfused with 300, 150 or 75 mM NaCl was 73.0 ± 2.2, 59.4 ± 1.5 and 42.6 ± 1.5 mV ($n = 7$), respectively. These reversal potentials were close to the theoretical Nernst equilibrium potentials for Na^+ under these conditions: 76.9, 59.2 and 41.4 mV, respectively (Fig. 2).

When the mean values of the reversal potential obtained at different values of $[Na^+]_o$ were plotted against the calculated theoretical sodium equilibrium potential, an apparently linear relationship was observed (correlation coefficient $r = 0.998$, $P < 0.05$), indicating that the currents were carried by sodium ions (Fig. 3).

3.3. Effect of TTX on the inward current

Repetitive single current traces were elicited for 20 ms in every 10 s until stable currents were recorded. We found that the amplitudes of the peak inward sodium currents were decreased progressively which reached a stable state in about 40 s after the external perfusion of TTX. Fig. 4 shows that TTX from 0.5 to 5 nM concentration-dependently decreased the peak values of the inward currents. Recovery was observed after washing out TTX from the

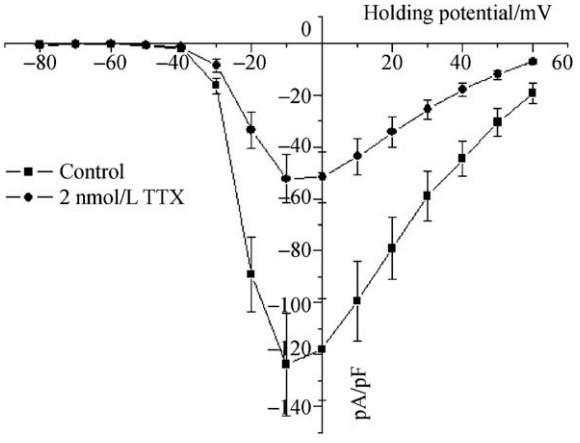

Fig. 1. TTX blocked the sodium currents in cells. Currents recorded every 10 s were obtained by a 20 ms step to test potentials between −80 and +60 mV with a holding potential of −70 mV. Macroscopic current values were normalized for cell capacitance as whole-cell current densities (pA/pF), which was plotted as a function against the membrane potentials in the absence (solid square) and presence of 2 nM TTX (solid circle). Each point represents the mean ± SE, which was obtained from five cells.

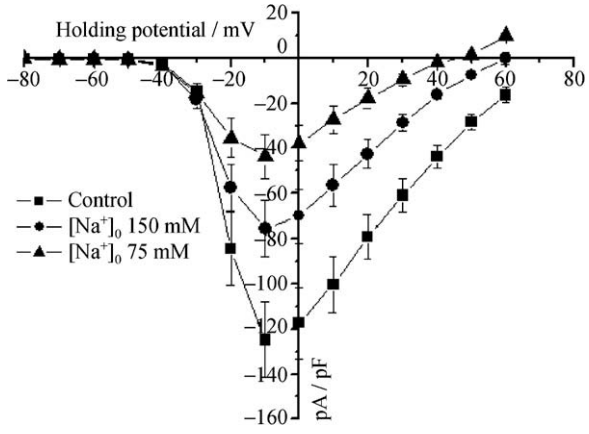

Fig. 2. Effect of changing $[Na^+]_o$ on the current–voltage relationship of the inward currents. External $[Na^+]$ was changed by replacing sodium chloride with equimolar choline chloride. Macroscopic current values were normalized for cell capacitance as whole-cell current densities (pA/pF), which were plotted as a function against the membrane potentials in the presence of 300, 150 and 75 mM $[Na^+]$. Each point represents the mean ± SE, which was obtained from six cells.

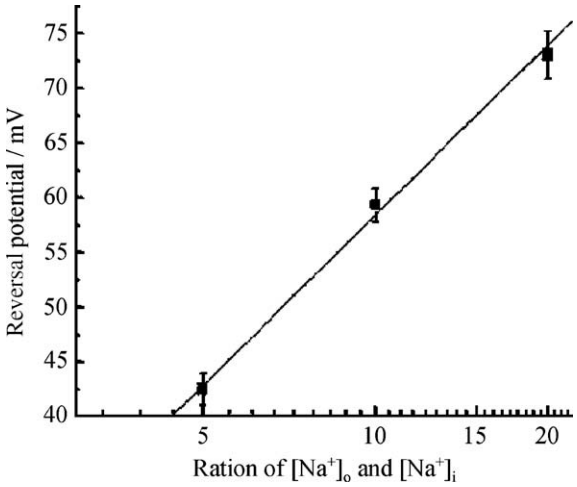

Fig. 3. Reversal potential of inward current, measured at three different external $[Na^+]$ (75, 150 and 300 mM), as a function of the ration of $[Na^+]_o$ and ($[Na^+]_i$). Data points are mean values observed in six cells. The solid line is the linear regression through the data points with a correlation coefficient $r = 0.998$, $P < 0.05$.

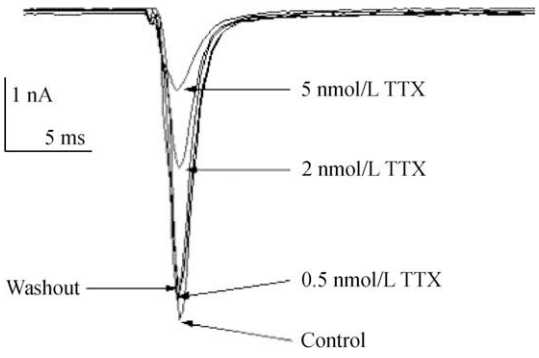

Fig. 4. TTX concentration-dependently blocked sodium currents. Currents were elicited by depolarization to −10 mV for 20 ms from a holding potential of −70 mV. Superimposed are currents from the same cell in the absence of TTX (control) and the presence of TTX which ranged from 0.5 to 5 nM.

external solution with fresh PSS. And the inward currents were always completely abolished at a TTX concentration above 30 nM.

Peak values of the inward current measured at the −10 mV test pulse from a holding potential of −70 mV were used as an index of inhibition, which were plotted as a function of TTX concentration (0.1–100 nM). The data were fitted with $I_{TTX}/I_{control} = 1/\{1 + (IC_{50}/[D])^n\}$, where [D] is the concentration of TTX used, IC_{50} is the concentration at half-maximal inhibition and n is the Hill coefficient. Fig. 5 shows that the effects of TTX on inward current were concentration dependent, with an IC_{50} of 2.1 ± 0.1 nM and n of 1.09.

3.4. Effect of TTX on the current–voltage relationship (I–V curves) of I_{Na}

Currents were evoked using the standard stimulus protocol. The membrane potentials were stepped for 150 ms

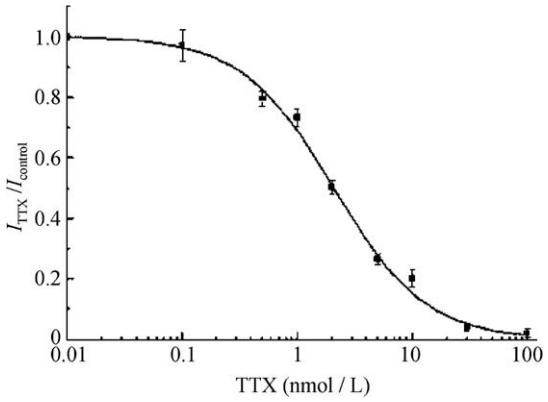

Fig. 5. Concentration-dependent inhibition of sodium currents by TTX. The amplitudes of the peak inward sodium currents were measured and normalized by control current amplitudes. The smooth line represents the best fitting with the Hill equation, which yielded an IC_{50} of 2.1 ± 0.1 nM and n of 1.09. Data are expressed as mean ± SE, $n = 3$–10.

from a holding potential of −70 mV to test potentials between −80 and +60 mV in 10 mV increments. The interval between two sweeps was set at 10 s to allow full recovery of inactivated channels. Peak currents of I_{Na} were measured at test pulses from −80 to +60 mV and macroscopic current values were normalized for cell capacitance as whole-cell current densities (pA/pF), which were plotted as a function of test pulses.

Fig. 1 shows that 2 nM TTX significantly blocked peak currents of I_{Na} over a wide range of test potentials between −80 and +60 mV ($P < 0.05$, $n = 5$). The threshold for activation of the sodium channel and the test potential to elicit peak current were unchanged. And the inhibition showed no voltage dependence.

3.5. Effect of TTX on voltage dependence of steady-state inactivation and activation

The classic double pulse protocol was used to determine the voltage dependence of inactivation of I_{Na}. Inactivation properties were studied by applying a conditioning pulse between −80 and 20 mV by an increment of 10 mV that was long enough (1 s) to allow the inactivation process to reach its steady-state level (Fig. 6). Thereafter, the membrane potential was stepped to −10 mV at which potential the inward current was almost maximal. The interval between two sweeps was set at 10 s. The inactivation curve, obtained by plotting normalized peak current (I/I_{max}) as a function of conditioning potentials, was fitted with a Boltzmann function: $I/I_{max} = 1/\{1 + \exp[(V_h - V)]/k\}$, where V is membrane potential, V_h is the half-maximal inactivation voltage and k is the slope constant (mV). TTX had no significant effect on the voltage dependence of steady-state inactivation of I_{Na}. Fig. 6 shows that the values of V_h were -44.2 ± 0.7 and -45.3 ± 0.7 mV ($P > 0.05$, $n = 6$), respectively, in the absence and presence of 2 nM TTX, the slope constants k were 4.4 ± 0.3 and 5.4 ± 0.7 mV, respectively ($P > 0.05$, $n = 6$).

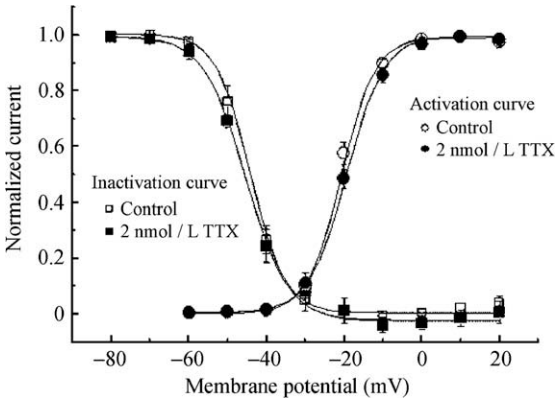

Fig. 6. Effect of TTX on steady-state activation and inactivation of sodium currents. Inactivation was shown as a plot of normalized peak current as a function of conditional potential from −80 to +20 mV. For voltage dependence of activation, normalized currents were calculated by dividing peak outward currents by their driving force and plotted against potential. Smooth curves were fitted with the Boltzmann equation which yields values of half-maximally activated or inactivated voltage (V_h) and slope constant (K). TTX has no significant effect on the voltage dependence of steady-state activation and inactivation of I_{Na}.

The voltage dependence of the TTX-sensitive inward current activation was also studied. The activation curves of I_{Na} were derived from I–V curves of I_{Na}, where G_{Na} were calculated by dividing the initial peak currents value by their driving force and plotted as a function of membrane potentials. The activation curves were fitted by a Boltzmann function $G/G_{max} = 1/\{1 + \exp[(V - V_h)]/k\}$, where V is the membrane potential, V_h is the half-maximal activation voltage and k is the slope constant (mV). TTX has no significant effect on the voltage dependence of steady-state activation of I_{Na}. Fig. 6, the values of the half-maximal activation voltage V_h were -20.6 ± 0.5 and -19.3 ± 0.5 mV, respectively, in the absence and presence of 2 nM TTX, ($P > 0.05$), the slope constants k were 4.4 ± 0.2 and 4.8 ± 0.3 mV, respectively ($P > 0.05$, $n = 6$). The overlap between the activation and inactivation curves in Fig. 6 suggests the possibility of Na^+ channel "windows current", i.e., there was a narrow range of membrane potentials, from about −40 to −20 mV, where some sodium channel could be open in the steady state.

4. Discussion

The experiments presented above are, to our knowledge, the first description of the properties of the TTX-sensitive inward current recorded from the carefully isolated neurosecretory cells in XOSG from the MTXO of *P. japonicus*.

Several lines of evidence in our investigation showed that the inward current recorded under our experimental conditions (i.e., in the presence of Ca^{2+} and K^+ channel blockers) was carried by sodium ions flowing through fast voltage-dependent Na^+ channels for the following reasons. (1) It had a rapid voltage and time-dependent rising (activation) and decay (inactivation) phase during depolarization. (2) In our experiment, it was concentration-dependently blocked by TTX (0.1–100 nM) with an IC_{50} of about 2 nM. The inward currents were completely blocked by TTX of a concentration above 30 nM. (3) Its reversal potential was very close to the Na^+ equilibrium potential, which was calculated from the Nernst equation when the Na^+ concentration in the bath solution was changed.

The electrophysiological properties and the sensitivity to TTX of the sodium channels in MTXO cells of *P. japonicus* are similar to those of other invertebrate neurons [20,21].

TTX, a toxin contained in the ovaries, eggs and liver of puffer fish, had proven to be a useful tool in the electrophysiological and molecular study of ion channels [22]. Voltage-sensitive sodium channels have been categorized as TTX sensitive (TTX-S) or resistant (TTX-R). The TTX-S sodium channel in various neuronal and muscle preparations are selectively and reversibly blocked by externally applied TTX, with nanomolar IC_{50} values in a one-to-one stoichiometric relationship.

In addition to these TTX-S sodium channels, TTX-R sodium channels with micromolar IC_{50} values have been found in neuron, denervated skeletal muscle and cardiac muscle preparations [23]. Electrophysiological analysis of TTX-R and TTX-S channels indicated that these channels differ in their activation and inactivation kinetics [23,24] and their interactions with externally applied divalent cations [25]. In our experiments, the IC_{50} for the TTX block of the sodium channel in the MTXO cells of *P. japonicus* was about 2.0 nM. The TTX-R sodium channel was not observed in our experiments, though the TTX-R sodium current was reported in many vertebrate nerve cells [26,27] and some crustacean preparation [28].

To check whether TTX could affect the biophysics kinetics of voltage-dependent sodium channels, we examined the steady-state activation and inactivation kinetics in the absence and presence of 2 nM TTX. We found that the TTX block did not alter the activation and inactivation kinetics of sodium channels, which agrees well with previous studies [29]. Evidence suggested that TTX binds as a plug to the extracellular mouth of the channel, blocking the flow of ions through the pore [30]. The lack of voltage dependence of the steady-state block implied that resting and inactivated channels bind toxin with virtually the same affinity and that the steady-state voltage dependence of inactivation is unchanged by the binding of toxin.

The primary function of sodium channels in most cells is to depolarize the membrane and generate the upstroke of the action potential. Although the sodium current in the soma of the X-organ neuron from *P. japonicus* is unknown yet, some hypothesis can be suggested. Intrasomatic recordings have shown that guinea pig (*Cavia porcella*) inferior olivary neurons, Purkinje and dorsal cochlear nucleus neurons are capable of generating spontaneously complex multiphasic or long duration action potentials composed of at least two distinct components, a fast sodium-dependent depolarization followed by a prolonged

slow calcium-dependent depolarization [31–33]. X-organ neurons are also capable of firing complex action potentials with a fast initial sodium-dependent depolarizing potential followed by a slow calcium-dependent depolarizing potential. The sodium spikes in the somata may act as a booster potential to activate the somatic calcium-dependent action potential which leads to an increase in internal Ca^{2+} so as to regulate secretion. Our work on the sodium current in somata of the MTXO cells does not correspond to previous studies on X-organ cells from crayfish [10]. Previous studies in the X-organ of the crayfish reported that the main inward current in the cell somata was due to Ca^{2+} and the control of spontaneous or evoked somatic electrical activity were elicited by neuritic sodium-dependent spikes. After proximal axotomy (150 μm from the soma), only a high threshold somatic slow calcium response could be elicited instead of a sodium/calcium action potential recorded *in situ*, suggesting that the spike activity was generated at the initial segment of the axon [28]. Using immunocytochemistry with antibodies raised against a specific peptide corresponding to regions of the sodium channel sequence. Sodium channels were identified in a large pool in the soma, though the density of staining was higher in the neurite and axon than in cell bodies [34–36]. Whether or not species difference contributed to the variation needs further investigation.

In conclusion, the present data reveal the presence of the voltage-gated sodium channel in somata of the MTXO cells from *P. japonicus*. The current is insensitive to Cd^{2+}, but sensitive to changes in $[Na^+]_o$, and it is blocked by TTX (above 30 nM) without modification of the property of its biophysical kinetics.

Acknowledgements

This work was supported by the National Natural Science Foundation of China (Grant No. 30300269) and the Technical Innovation Project of Fujian (Grant No. 2003J018). We are thankful to Prof. Paul K. Chien, Department of Biology, University of San Francisco, for his detailed comments and fruitful suggestions.

References

[1] Bliss DE, Welsh JH. The neurosecretory system of brachyuran Crustacea. Biol Bull 1952;103:157–69.
[2] Garcia U, Arechiga H. Regulation of crustacean neurosecretory cell activity. Cell Mol Neurobiol 1998;18(1):81–99.
[3] Beltz SB. Crustacean neurohormones. In: Invertebrate endocrinology (endocrinology of selected invertebrate types). New York: AR, Liss; 1988. p. 235–58.
[4] Keller R. Crustacean neuropeptides: structures, functions and comparative aspects. Experientia 1992;48:439–48.
[5] Fingerman M, Nagabhushanam R, Sarojini R. Vertebrate-type hormones in crustaceans: localization, identification and functional significance. Zool Sci 1993;10:13–29.
[6] Farfante IP, Kensley B. Penaeid and sergestoid shrimps and prawns of the world. Keys and diagnoses for the families and genera. Mém Mus Natn Hist Nat 1997;175:1–233.
[7] Dall W, Hill J, Rothlisberg PC, et al. The biology of Penaeidae. In: Advances in marine biology, vol. 27. London: Academic Press; 1990. p. 1–489.
[8] Huang JQ, Lin QW. Factors affecting molting of *Penaeus japonicus* parents. Mar Sci 1992;17(2):30–1, [in Chinese].
[9] Lapied B, Malecot CO, Pelhate M. Patch–clamp study of the properties of the sodium current in cockroach single isolated adult aminergic neurons. J Exp Biol 1990;151:387–403.
[10] Cooke I, Graf R, Grau S, et al. Crustacean peptidergic neurons in culture show immediate outgrowth in simple medium. Proc Natl Acad Sci USA 1989;86:402–6.
[11] Lara J, Acevedo JJ, Onetti CG. Large-conductance Ca^{2+}-activated potassium channels in secretory neurons. J Neurophysiol 1999;82(3):1317–25.
[12] Zhao X, Sun JS, Zhang ZY. Studies on calcium-activated potassium channel expressed by the neurosecretory cells of medulla terminalia X-organ in the eyestalks of *Eriocheir sinensis*. J Fish China 2007;31(4):417–22, [in Chinese].
[13] Duan S, Cooke IM. Selective inhibition of transient K^+ current by La^{3+} in crab peptide-secretory neurons. J Neurophysiol 1999;81:1848–55.
[14] Martinez JJ, Onetti CG, Garcia E, et al. Potassium current kinetics in bursting secretory neurons: effects of intracellular calcium. J Neurophysiol 1991;66:1455–61.
[15] Garcia E, Benitez A, Onetti CG. Responsiveness to D-glucose in neurosecretory cells of crustaceans. J Neurophysiol 1993;70:758–64.
[16] Onetti CG, Lara J, Garcia E. Adenine nucleotides and intracellular Ca^{2+} regulate a voltage-dependent and glucose-sensitive potassium channel in neurosecretory cells. Pflügers Arch Eur J Physiol 1996;432:144–54.
[17] Sun JS, Gao CL, Xiang JH. Study on the GABA gated channels in the neurosecretory cells of MTXO in the eyestalks of *Eriocheir sinensis*. Prog Biochem Biophys 2003;30(1):129–33, [in Chinese].
[18] Catterall WA. Cellular and molecular biology of voltage-gated sodium channels. Physiol Rev 1992;72:15–48.
[19] Lang GH, Nomura N, Matsumura M. Growth by cell division in shrimp (*Penaeus japonicus*) cell culture. Aquaculture 2002;213:73–83.
[20] Davis RE, Stuart AE. A persistent, TTX-sensitive sodium current in an invertebrate neuron with neurosecretory ultrastructure. J Neurosci 1988;8:3979–91.
[21] Liu ZQ, Song WZ, Dong K. Persistent tetrodotoxin-sensitive sodium current resulting from U-to-C RNA editing of an insect sodium channel. Proc Natl Acad Sci USA 2004;101(32):11862–7.
[22] Narahashi T. Chemicals as tools in the study of excitable membranes. Physiol Rev 1974;54:813–89.
[23] Roy ML, Narahashi T. Differential properties of tetrodotoxin-sensitive and tetrodotoxin-resistant sodium channels in rat dorsal root ganglion neurons. J Neurosci 1992;72(6):2104–11.
[24] Schwartz A, Palti Y, Meiri H. Structural and developmental differences between three types of Na channels in dorsal root ganglion cells of newborn rats. J Membr Biol 1990;116:117–28.
[25] Roy ML, Narahashi T. Effects of saxitoxin, divalent cations and lidocaine on tetrodotoxin-sensitive and tetrodotoxin-resistant sodium channels in rat dorsal root ganglion neurons. Biophys J 1991;59:263.
[26] Onetti CG, Garcia U, Valdiosera RF, et al. Ionic currents in crustacean neurosecretory cells. J Neurophysiol 1990;64:1514–26.
[27] Blair NT, Bean BP. Roles of tetrodotoxin (TTX)-sensitive Na^+ current, TTX-resistant Na^+ current, and Ca^{2+} current in the action potentials of nociceptive sensory neurons. J Neurosci 2002;22(23):10277–90.
[28] Tripathi PK, Trujillo L, Cardenas CA, et al. Analysis of the variation in use-dependent inactivation of high-threshold tetrodotoxin-resistant sodium currents recorded from rat sensory neurons. Neuroscience 2006;43(4):923–38.
[29] Cohen CJ, Bean BP, Colatsky TJ, et al. Tetrodotoxin block of sodium channels in rabbit Purkinje fibers. J Gen Physiol 1981;78:383–411.
[30] Hille B. The receptor for tetrodotoxin and saxitoxin. Biophys J 1975;15:615–9.

[31] Mcmanus OB. Calcium-activated potassium channels: regulation by calcium. J Bioenerg Biomembr 1991;23:537–60.
[32] Petersen OH, Maruyama Y. Calcium-activated potassium channels and their role in secretion. Nature 1984;307:693–6.
[33] Ewer J, Gammie SC, Truman JW. Control of insect ecdysis by a positive-feedback endocrine system: roles of eclosion hormone and ecdysis triggering hormone. J Exp Biol 1997;200:869–81.
[34] French AS, Sanders EJ, Duszyk E, et al. Immunocytochemical localization of sodium channels in an insect central nervous system using a site-directed antibody. J Neurobiol 1993;24:939–48.
[35] Seyfarth EA, Sanders EJ, French AS. Sodium channel distribution in a spider mechanosensory organ. Brain Res 1995;683:90–101.
[36] Johnston WL, Dyer JR, Castellucci VF, et al. Clustered voltage-gated Na channels in Aplysia axons. J Neurosci 1996;16:730–9.